Available online at www.sciencedirect.com

jmr&t Journal of Materials Research and Technology

journal homepage: www.elsevier.com/locate/jmrt

Original Article

Analysis of biomedical titanium implant green parts by X-Ray tomography

Levent Urtekin [a,*], *Fatih Bozkurt* [b], *Murat Çanli* [c]

[a] *Kırşehir Ahi Evran University, Mechanical Engineering Department, 40100, Kırsehir, Turkey*
[b] *Eskisehir Technical University, Vocational School of Transportation, 26470, Eskisehir, Turkey*
[c] *Kırşehir Ahi Evran University, Mucur Vocational School, Department of Chemistry and Chemical Processing Technologies, 40500, Mucur, Kırşehir, Turkey*

ARTICLE INFO

Article history:
Received 12 May 2020
Accepted 23 June 2021
Available online 29 June 2021

Keywords:
Implant
Green part
X-ray tomography
Powder injection molding

ABSTRACT

In this study, X-ray tomography was applied as a non-destructive test to investigate the internal defects of the green part produced with Powder injection molding (PIM). PIM is a material processing technology that combines injection molding with powder metallurgy. The determination of multiple parameters such as rheology, molding, bonding, and sintering stages in the PIM method requires a long time, energy, and high cost. Metal and ceramic injection molded parts are known to be susceptible to defects like cracks, weld lines, bubbles, or gaps. The examination and elimination of these defects are critical to the safety of the products because even a very short crack can significantly reduce the tensile and fracture strength of the parts. The internal structure analysis of the green parts after molding is very difficult. Defects (internal cracks, micropores, jetting, etc.) occurring in the green part will occur in the sintered. Therefore, it is essential to analyze the possible defects on molded parts before applying the ongoing process to save time and costs. Since the medical implants are in complex shape in general, the more internal defects can be seen at molding stage, it is needed to check the internal structure without any destruction, because there is no chance toleave them for recycle in the case of any defect. In experimental studies, it was observed that there were defects of edge, interior, and gaps in X-ray analysis for four different injection parameters. In X-ray analysis, the defects free parts were obtained for green part 4 parameters (temperature of 237 °C, flow rate of 20.11 cm^3/s and pressure of 120 MPa). As a result of X-ray analysis, the difference between green part 1 and green part 4 is clearly visible in terms of defect. Injection temperatures, speeds and pressure play important role on originating of defects.

* Corresponding author.
E-mail address: levent.urtekin@ahievran.edu.tr (L. Urtekin).

https://doi.org/10.1016/j.jmrt.2021.06.083

1. Introduction

The technology of the powder injection molding (PIM), in specific the metal injection molding (MIM), combines the plastic injection and powder metallurgy. It has capable of producing intricate and small parts that almost have near-net-shape for highly automated mass production purposes [1–6]. Up to now, it has been found that biocompatible metals are the most desirable materials for commercial medical implants due to their excellent mechanical, physical and chemical properties. In addition to that, PIM technology has been extensively used in the production of the component in the medicine field such as surgery and dentistry [7–9]. In the past, the main criteria for choosing the implant material were suitable physical properties and non-toxicity. But recent expectation is to include some properties such as assisting in the growth of human body tissues and outstanding properties. The most extensively used implant materials for biomedical applications are stainless steel, titanium, and cobalt-based alloys. These materials are chosen due to their superior mechanical, chemical properties, and corrosion resistance as well. Among them, titanium alloys, especially "Ti6Al4V alloy", are extensively used because of its superior heat resistance, strength, plasticity, toughness, formability, weldability, corrosion resistance, and biocompatibility. Due to their unique properties such as lightweight and higher specific strength, it is also extensively used in the aerospace industry [10].

PIM is one of the productional techniques for the application of titanium and its alloys in the medical industry. The four main steps in PIM technique to produce a part are; 1) mixing, 2) injection molding, 3) debinding and 4) sintering [11–13]. The parameters which affected the quality of mold filling are injection pressure, speed, and temperature. If these parameters are not chosen properly, it might lead to the formation of defects in the green part. The main disadvantage of PIM method is that there might be porosity or cracks in the structure of the green part after forming. Almost all production methods, not only PIM technology, the presence of any defects or flaws have a negative effect on mechanical properties of the final part and it can cause catastrophic cases due to exhibiting lower mechanical properties. In order to minimize the undesirable situation, the production methods must be improved continuously [14]. Due to difficulties in determining defects such as pore and microcrack during the production of green parts, destructive examinations (tensile test, 3-point bending testing, SEM) are used on sintered parts and those tests show only external defects. The other methods such as the ultrasonic test methods cannot show internal defects directly and the eddy current method does not give the detail of the fault. The conventional observation techniques i.e., scanning electron microscope and optical microscope need the process of sample preparations such as cutting and polishing. During sample preparation steps, many errors can occur, and artificial defects can change the original structure of the sample. Also, due to the low strength of the injected green part, powders can be pulled out and binder can smear onto the surface. Therefore, the internal structure analysis is difficult and it is not suitable to perform the detection of defects in the green part [15–18]. Thanks to new characterization techniques like X-ray tomography (it is also known as X-ray micro-computed tomography or computed tomography) is applied to fields of material science and it enables to get 3D information about the inner structure of the final product without destroying. With this method, it is possible to detect the size and the location of the defect at high resolution [19–25].

In the literature of the injection process, Qu et al. studied 6061 aluminum alloy and 316L stainless steel green parts produced by different injection parameters such as injection pressure, speed, and temperature [15]. The green bodies were analyzed by X-ray tomography, after the completion of the injection process and the different types of defects were obtained by the improper injection parameters. The spatial morphology characteristics of the serious defects were demonstrated by using 3D rendering of the green parts. The reasons of the defect formation were tried to understand, and the optimization of the injection parameters was performed for stainless steel and aluminum alloy. Weber et al. investigated the effect of the powder distribution (stainless steel 17–4 PH) in green parts with respect to the molding parameters using synchrotron microtomography and 3D image evaluation [26]. They concluded that the microtomography was a key tool for investigating the powder distribution in micro-powder injection molding process. Hedele et al. used X-ray tomography for the particle distribution of ceramic powders in thermoplastic binders to determine the particle density and defect distribution in micro parts [27]. Their results showed that the crucial defects and density variations can be detected, and the injection molding process can be optimized using X-ray tomography. Xinbo et al. focused on the influence of filling patterns on the powder-binder separation in PIM [28]. Using X-ray CT, the powder-binder separation was detected for the green part. By the evolution of powder-binder separation obtained by numerical simulation, the experimental phenomena were explained in detail. In summary, X-ray imaging is a promising method for non-destructive testing and quality control for PIM and MIM parts. Another advantage of the method is that all examination procedures can be performed within seconds, and this allows routine and serial testing of all manufactured parts in a production line. Various defects affecting the mechanical properties of the products in the sintered state, such as glare, distortion or edge rounding, can be detected by X-ray tomography in the green parts of smaller sizes than millimeters. Wall shift, surface roughness or jetting effects on the flow behavior of micro-size green material systems can be visualized by X-ray tomography and may serve as a reference for further research. To obtain a better resolution on X-ray tomography, different powder materials with different particle sizes or other tomography modes like phase contrast can be used.

In comparison with other biocompatible metals such as stainless steel and cobalt-base alloy, titanium and its alloys have exhibited perfect biocompatibility and outstanding mechanical properties which are close to the bone. The passive oxide layer formed on the surface protects titanium implant material against pitting corrosion and intergranular corrosion [10,29–33].

The difficulties in the machining of titanium alloy leads to use PIM on the production of cortical bone screw. In

Table 1 – Chemical compositions and mechanical properties of the Ti_6Al_4V titanium alloy.

Element	Weight %	Atomic %
Al K	6.30	10.68
Ti K	90.26	86.23
V K	3.44	3.09

comparison to the other steels and alloys, titanium alloys need higher cutting force during the machining process. Another disadvantage of titanium alloys, despite having almost equal hardness with other alloys, the metallurgical properties make the alloy difficult to machine or process. Realistic processing rates of machinability can be achieved at an acceptable cost level, if the processing conditions are selected for a particular alloy composition and type of machining. More recent attention has focused on the development of new tool materials for the improvement of the machining of titanium alloys [29,30]. Because of the difficulties in the machining of Ti_6Al_4V implant, as well as intensive use in both hip and wrist, mass production of these medical parts is required.

X-ray tomography is a commonly used tool within the materials science research efforts for enlightening of solid parts of a material [34–36]. Thanks to the X-ray tomography, the re-use or recycling of defective green parts produced with PIM method will be easier than the pressed part since the feedstock consists of the thermoplastic binder. Material, energy and time can be saved by determining the porosity and microcracks of the green part before starting the process of the sintering. X-ray tomography was used as a non-destructive examination method to analyze the internal defects of the green part produced with PIM, to investigate the causes of these defects and to produce solutions to prevent them.

The most important factor that distinguishes the study from other similar studies is that the feedstock is produced by the researchers, and it is easier to eliminate rheology-related errors [37,38]. In addition, another important difference is that a workflow chart has been created and the applicability of X-Ray tomography, which is generally applied to powder metal parts, with flow simulation program to powder injection molding has been investigated. With the latest developed

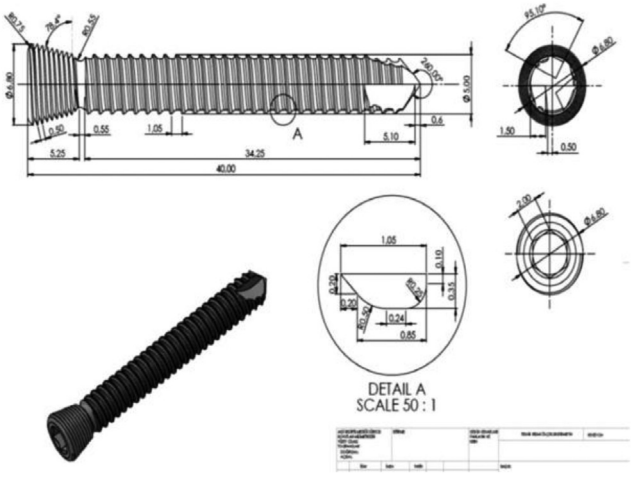

Fig. 2 – Cortical-bone screw-implant design [1].

programs, such as Moldflow (metal thinning molding), it has been made suitable and more realistic results.

2. Experimental procedure

2.1. Materials

The samples used in the study were prepared from powder injection molding Ti_6Al_4V material. The chemical composition and mechanical properties of the Ti_6Al_4V titanium alloy are shown in Table 1. Average particle size: 13.4 micron and the powder form is to be spherical.

The results of cast Ti_6Al_4V energy dispersive X-ray spectroscopy (EDS) analysis performed by JEOL JSM-6360 LV electron microscope are given in Fig. 1. According to Fig. 1, the highest peaks appear to be titanium, aluminum, and vanadium, respectively.

2.2. Homogenity mixing

The study includes the binding system consisting of PP/PEG/SA. First, the binders and then the Ti_6Al_4V powders were

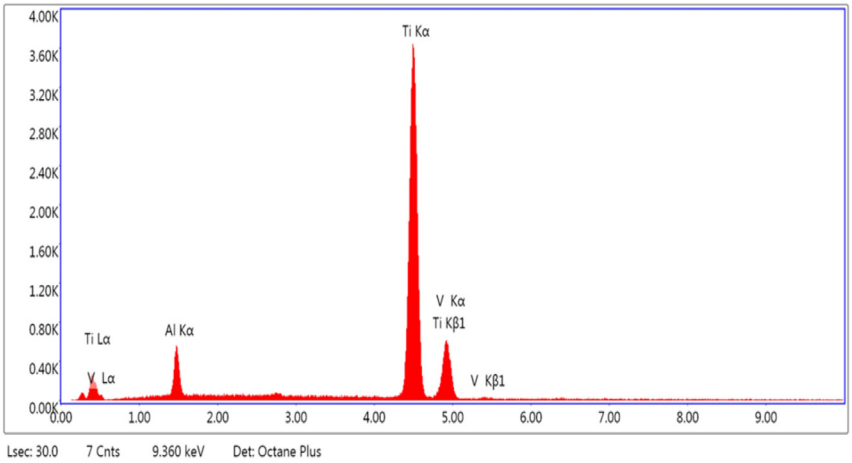

Fig. 1 – EDS analysis of Ti alloy.

Fig. 3 – SEM ve X-RAY Tomografi cihaz görüntüleri.

mixed with the binder system in a dry environment in certain proportions for about 45 min. Thus, 100 cm^3 feedstock mixes were prepared. Feeding stocks were turned into granules by using an extruder. To prevent the formation of air bubbles, a continuous vacuum was made in the area close to the mold part during granulation. Air bubbles or granules that will form in the granule appear as cavities during molding. The typical grain (granule) size is 4 mm.

2.3. *Injection molding parameters*

In Fig. 2, implant geometry produced by injection molding is given. 3D solid models of designs were obtained by the reverse engineering method. The cortical bone screw used in the application (hospitals) was scanned with a laboratory scanning device and an implant designed for one-to-one working was designed. In the Powder Injection method, as a result of removing the binders in the feedstocks, a shrinkage of 17–20% occurs in the green parts. This detail was taken into account during the mold design. The cortical-bone screw-implant, whose preliminary designs are given in Fig. 3, has been designed with SOLIDWORKS.

Injection parameters were used in various trials to produce the implant. Injection parameters were used in various trials to produce the implant. Flow rate, pressure, temperature, clamping force, die filling time and holding pressure are given in Table 2.

2.4. *SEM analyses and X-Ray tomography*

SEM analyses was performed using Hitachi Regulus 8230 scanning electron microscopy (SEM) after granulation. After injection process, images were captured from SEM with 30× magnification for surface roughness and 2000× magnification for micro-cracks. According to ASTM E2869 standard, YXIon X-Ray unit was used to detect the pores and gaps formed in the samples. X-Ray tomography (minimum power 85 kW and 0.05 A) images were taken for Ti alloy samples with different parameters. The experiments were carried out to perform X-ray tomographic scanning for samples obtained using an injection pressure of 100 MPa, a velocity of 50 cm3/s and a temperature of 165 °C. Fig. 3 shows the SEM and X-Ray device images used in the experiments.

3. Experimental results

As shown in Fig. 4, the binders form a film layer on the powders during the powder/binder mixture. This formed film layer plays an important role in determining the injection temperature during injection molding. In addition, the binders used to determine the flow characteristics of the feedstock consisting of powder/binder. In short, the coating or film layer formed by the binder is decisive in the injection molding and subsequent de-binding process.

The rheology experiments were carried out on the granules obtained homogeneously. Rheological experiments of powder loading were performed in the volumes of 50–60%. The melting flow index change is in the range of 261–1888 (gr/10 min). On the other hand, the viscosity change is between 72 and 1001 Pa and it is in the ideal ratio. When the viscosity-temperature graph is examined, it is seen that the viscosity values are below 1000 Pa. Flow type is pseudo-plastic, that is, viscosity decreases with temperature. As a result of rheology experiments, it can be said that the feedstock is suitable for injection molding both in terms of volumetric loading ratio (%60), melt flow index and viscosity-temperature variation [39,40]. The feedstocks obtained with PP/PEG/SA were determined as 60% optimum loading by volume and after that the molding process was started. In Fig. 5, the molded part and mold design are depicted.

Table 2 – Parameters of injection molding.

Properties	GreenPart 1	GreenPart 2	GreenPart 3	GreenPart 4
Flow rate (cm^3/s)	16.92	17.95	18.91	20.11
Pressure (MPa) Max	100	105	110	120
Temperature (°C) Max	215	220	225	237
Close force (ton) Max	1700	2000	2500	3200
Holding pressure (MPa) Max.	34.83	38.94	42.7	47.1

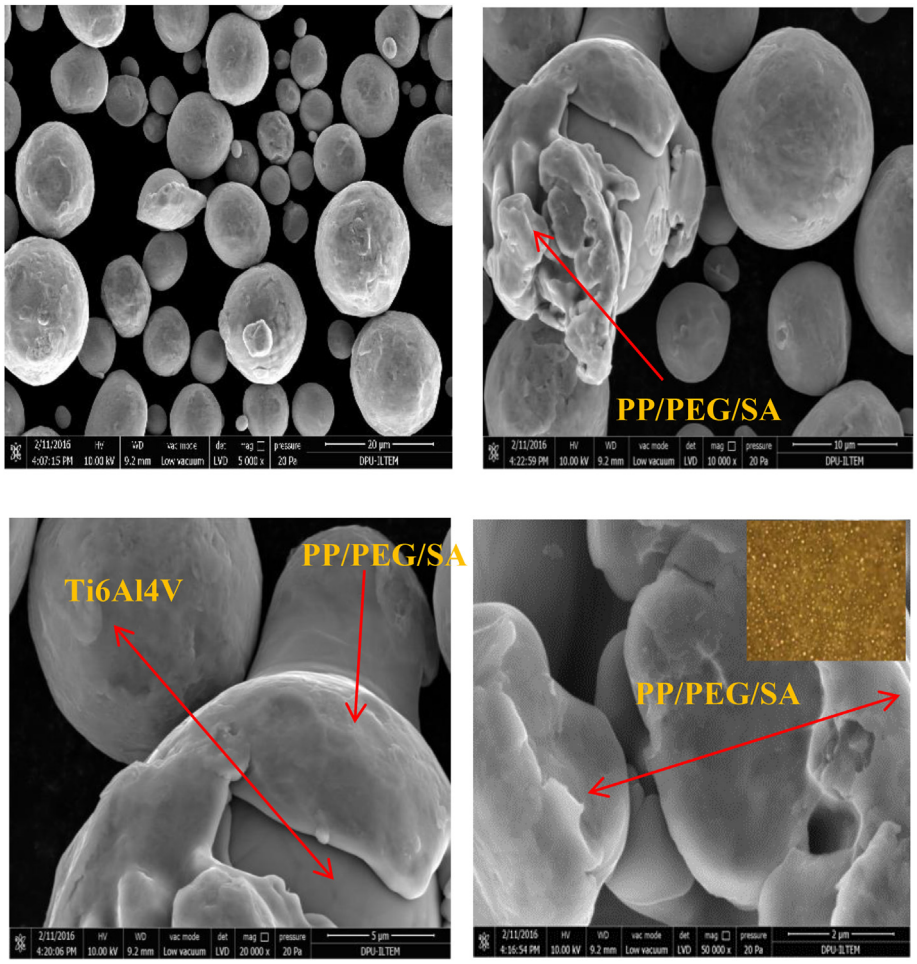

Fig. 4 – SEM of the cover of the binder to coat the dust and form a thin film layer.

In Fig. 6, the green part image is given for high pressure (120–155 MPa) applications. It was observed that the green part preserved its geometry at 120 MPa pressure value and over 120 MPa the problems occurred such as removal from mold and flash. In here, there are two main factors play critical role, the first one is molding pressure and the second one is holding pressure. The holding pressure was maintained to be 30% of the injection pressure. Therefore, the problem occurred due to the high injection pressure.

Images of green parts produced in different parameters were taken with the X-ray tomography device. In the images are given in Fig. 7, damage to the green part can be seen after X-ray shooting. Images were taken for four different molding

Fig. 5 – Green part production with 60% feedstock by volume.

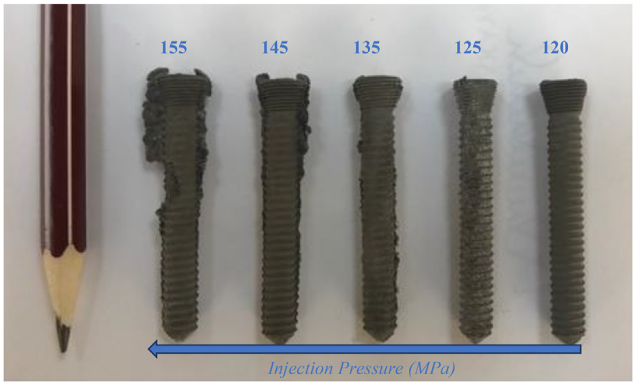

Fig. 6 – Molding of the green part in high pressure applications.

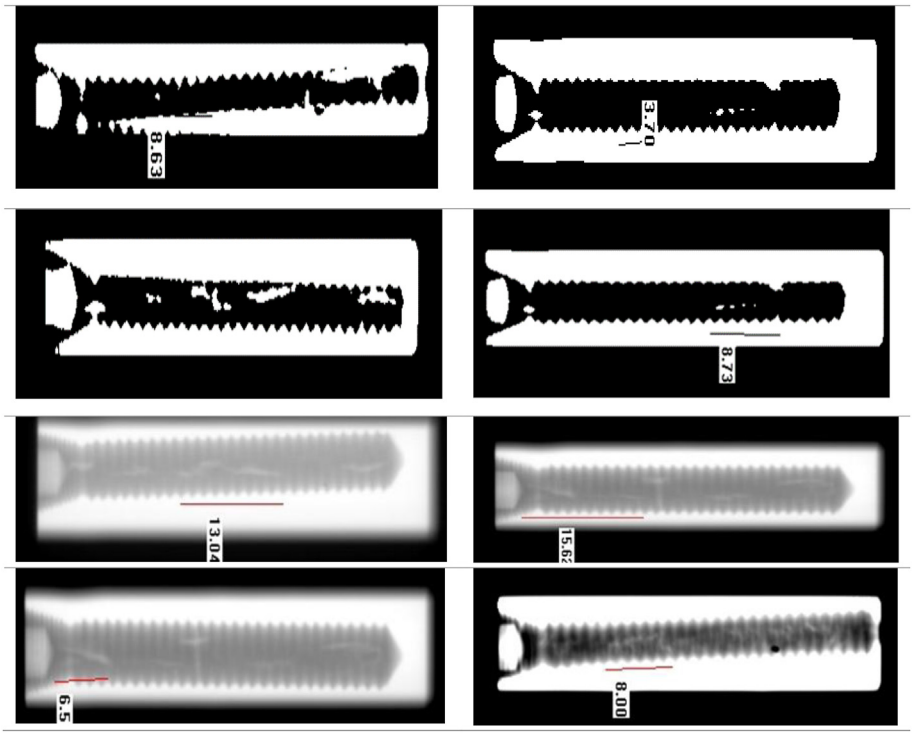

Fig. 7 – X-ray tomograhy analysis of the green part produced with different parameters.

parameters. As a result of x-Ray analysis, the crack formed near the mold boundary (edge), the cracks appearing in the central part and internal gaps were determined in the parts. If most of the errors in injection molding are not due to rheology, injection pressure, temperature, and flow rate are caused. At high injection pressures, jetting and burr formation, low injection pressures, mold filling, and incomplete filling occur. At high temperatures, it is not possible to reuse the granule since the decomposition process will begin.

As can be seen in Fig. 7, parameters such as flow rate, pressure, temperature, holding pressure and time have been changed and the most suitable injection molding parameters have been determined. It can be said that an ideal molding was performed for Green part 4 and it is also in harmony with the simulation study applied for two-eyed and four-eyed molding operations [1,40]. As a result of X-ray analysis, it was observed that there were edge and middle defects in the green part. As seen in Fig. 7, severe defects are shown for four different groups. This study was performed to compare green parts obtained with different injection parameters (injection temperature, injection pressure and speed). As the injection pressure and temperature increase, the amount and average volume of large pores decreased. Furthermore, increased temperature has more pronounced effects to reduce injection defects. Therefore, an increase in temperature is an effective way to obtain appropriated injection parameters. For these injection parameters, the main defects are cracks which are seen in the middle region. In Fig. 7, it is clearly seen that the pores (gaps) and cracks in the middle region gradually disappear as the temperatures increases from 215 °C to 237 °C. It is possible to obtain appropriate injection parameters using X-ray tomography. Lower injection pressure and speed can

Table 3 – Types of defects according to different parameters according to x-ray tomography analysis.

Properties	GreenPart 1	GreenPart 2	GreenPart 3	GreenPart 4
Parameters	T ↓	T ↓	T ↓	✓T
	P ↓	P ↓	P →	✓P
Result	the cracks of edge the craks of interior pore	the craks of interior pore	the cracks of edge	minimum flaw

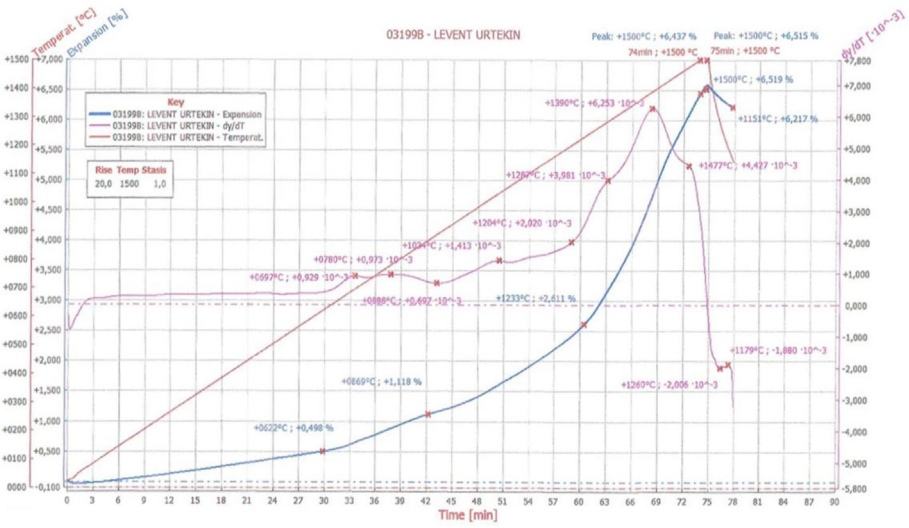

Fig. 8 – pVT analysis for the green part.

Fig. 9 – The Green part solvent debinding.

reduce the mold removal force and powder-binder separation, respectively. Small cracks were observed at the bottom of the green parts. If the injection speed or temperature is too high, it causes the phenomenon called as jetting. The parameters which are used for green part 1 (Pressure-Temperature-Flow Rate), large pores are formed in the parts. In Fig. 7, the defect between green part 1 and green part 4 can be seen in prominently. Table 3 summarizes the situation showing the effect of temperature and pressure changes on defect formation.

Debinding process was performed on the defect free samples which are scanned on X-ray tomography. If the parts have some defects, they are recycled for granulation process. The debinding step for PIM is an important process and it is done in two ways depending on the type of debinding. Solvent and thermal debinding. Thermal debinding parameters (speed and temperature) were carried out in line with the data obtained by thermal analysis. Binder distortion temperature, flash temperature, melting temperature, etc. DTA, TGA and pVT analyses were performed to determine the temperature ranges that should be known in this respect. Binder removal was carried out in a protective atmosphere furnace. Debinding was performed in two steps depending on the binder, solvent removal, and thermal decomposition. PEG8000, a water-based binder, was removed by leaving it in heated water at 60 °C for 24 h. Thermal decomposition was performed at heating rates of 1 °C/min under a protective atmosphere (Ar) based on TG analysis. Heating rate was applied as 5 °C/min and the temperature was increased to 600 °C. As a result of thermogravimetric analysis, it was determined that the initial sample deteriorated at 240 °C. In Fig. 8, pVT analysis curve is given.

The purpose of pVT analysis is to obtain the data required to examine the temperature and pressure changes that occur during injection molding. Values such as heat capacity, thermal conductivity feature and specific heat of the ideal feedstock are important for injection molding pVT analysis was used. Since each mixture will exhibit a different flow characteristic, the change of feedstocks with temperature and pressure is an important criterion. As a result of pVT analysis, PEG which is water soluble, was left to dissolve in heated water at 60 °C for 24 h. In Fig. 9, the samples are shown after debinding process and it is seen that there is no deformation has occurred.

Thermal debinding was conducted at 1 °C/min heating rates under a protective atmosphere (Ar) and the temperature increased to 900 °C. In Fig. 10, it is seen that the samples have not deformed after thermal debinding process. In the Ti_6Al_4V alloy powder injection process, the different kinds of defects emerged due to the improper injection parameters (injection

Fig. 10 – The green part of termal debinding.

pressure, flow rate and temperature). X-ray tomography was successfully applied to detect these defects in the green bodies. Due to the low injection temperature (210 °C and 220 °C), many big pores and cracks emerged in the green bodies. As the injection pressure and speed increase (120 MPa and 237 °C), the amount and average volume of the big pores decreased. For Green part 4, the cracks occurred mainly near the mold boundary and apparent pores and cracks disappeared in the central region compared to cases obtained with low injection temperatures (210 °C and 220 °C). Injection parameters applied for Green part 4 appear to be the most suitable injection parameters for Ti_6Al_4V alloy. Due to the jetting phenomenon, serious defects (large pores) have appeared in the green parts with high injection pressure (>120 MPa) and speed (>20 cm^3/s). When Ti_6Al_4V alloy is produced with the powder injection molding injection method, appropriate injection parameters are obtained very efficiently using X-ray tomography. Green part 4 parameters were verified by X-ray tomography analysis for injection molding and defect free part production in samples obtained by optimum powder loading rate determined in the volume of 60%. In traditional studies with injection molding parameters, numerous of experiments must be made. In addition, the defects in the internal structure of the part are determined by destructive inspection methods after sintering process. It is understood that internal structure analysis of the green part can be determined properly with the X-ray analysis method before sintering. After X-ray analysis, the thermal and solvent debinding operations were carried out considering pVT analysis. It is possible to obtain defect free part production with X-ray tomography.

4. Conclusion

The main principle in the study is to ensure the control of the green part without going through the sintering phase. By adding Moldflow analysis and X-ray tomography mechanisms to the classical powder injection molding system, the sintering of the defect-free part is aimed. First of all, the lower limit parameters to be used in injection molding were determined by Moldflow simulation. These parameters are determined as flow rate, pressure, temperature, holding time and holding pressure. In the literature, it has been determined that as a result of the experience gained by using destructive inspection methods (SEM, optics), large pores and cracks occur at low temperatures and large pores decrease with increasing injection pressure.

At high injection speeds and pressures, jetting (large pore) occurred in the green part and can be determined by SEM analysis. At high debinding rates, superficial cracking, and failure of the part to maintain its shape, plastering of the binder to the sample, and distortion occur. Since the binder forms a thin film layer on the powders, the pore between the dust and binders is almost nonexistent. Therefore, errors caused by injection parameters were more obvious (internal and superficial crack, large pore, open-closed pore, jetting, etc.) and selectable. The errors associated with these injection parameters should be more selectable (internal and superficial cracks, large pores, open closed pores, jetting, etc.). As a result of these experiences, the effects of changes such as X-ray tomography analysis (non-destructive examination), injection pressure, speed and temperature, connector removal rate temperature and waiting times on the part were examined. Qu et al. performed an X-ray analysis of the green parts they obtained with Al6061 and 316 Stainless steel powder in their study [15]. They examined the changes in pressure, speed, and temperature changes in the green part as injection parameters. In the study conducted by Muchavi et al. [41], it was mentioned that X-ray tomography of powder injection and powder rolling parts was used, and it was mentioned that the non-destructive inspection measurement was very useful. With the help of X-ray tomography, cracks and error analysis of the green parts were made and recycling of the thermoplastic-based feedstocks was provided by recycling. Another advantage of the method is that it can be applied to any PIM part. In industrial applications, since the system will be integrated directly into the production line, it will be possible to detect faulty parts in real-time.

The defects that occur in the raw part cannot be removed by sintering. It has been observed that the resulting defects would be eliminated if appropriate injection parameters are used. As a result of the sintering of parts with serious defects, it is understood that the faults cannot be eliminated. In defect-free samples produced with appropriate injection molding, parts close to full density are obtained. The aim of the study was succeeded that the errors caused by injection have been minimized to convert the thermoplastic-based feedstocks into granules and make injection molding again without going to the sintering stage [42,43].

Declaration of Competing Interest

The authors declare that they have no known competing financial interests or personal relationships that could have appeared to influence the work reported in this paper.

Acknowledgment

Part of this work was supported by the Scientific and Technological Research Council of Turkey (TUBITAK) with grant number 114M766.

REFERENCES

[1] Urtekin L, Genç A, Bozkurt F. Fabrication and simulation of feedstock for titanium-powder injection-molding cortical-bone screws. Mater Tehnol 2019;53(5):619–25.
[2] Bolzoni L, Ruiz-Navas EM, Gordo E. "Feasibility study of the production of biomedical Ti–6Al–4V alloy by powder metallurgy. Mater Sci Eng C 2015;49:400–7.
[3] Liu D-M. Influence of solid loading and particle size distribution on the porosity development of green alumina ceramic mouldings. Ceram Int 1997;23(6):513–20.
[4] Liu Y, Li K, Luo T, Song M, Wu H, Xiao J, et al. "Powder metallurgical low-modulus Ti–Mg alloys for biomedical applications. Mater Sci Eng C 2015;56:241–50.
[5] Mannschatz A, Höhn S, Moritz T. Powder-binder separation in injection moulded green parts. J Eur Ceram Soc 2010;30(14):2827–32.
[6] Choi J-P, Lee G-Y, Song J-I, Lee W-S, Lee J-S. "Sintering behavior of 316L stainless steel micro–nanopowder compact fabricated by powder injection molding. Powder Technol 2015;279:196–202.
[7] Torres Y, Lascano S, Bris J, Pavón J, Rodriguez JA. Development of porous titanium for biomedical applications: a comparison between loose sintering and space-holder techniques. Mater Sci Eng C 2014;37:148–55.
[8] Rivard J, Brailovski V, Dubinskiy S, Prokoshkin S. Fabrication, morphology and mechanical properties of Ti and metastable Ti-based alloy foams for biomedical applications. Mater Sci Eng C 2014;45:421–33.
[9] Gemelli E, de Jesus J, Camargo NHA, de Almeida Soares GD, Henriques VAR, Nery F. Microstructural study of a titanium-based biocomposite produced by the powder metallurgy process with TiH2 and nanometric β-TCP powders. Mater Sci Eng C 2012;32(4):1011–5.
[10] Hamidi MFFA, Harun WSW, Samykano M, Ghani SAC, Ghazalli Z, Ahmad F, et al. A review of biocompatible metal injection moulding process parameters for biomedical applications. Mater Sci Eng C 2017;78:1263–76.
[11] Ramli MI, Sulong AB, Muhamad N, Muchtar A, Zakaria MY. Effect of sintering on the microstructure and mechanical properties of alloy titanium-wollastonite composite fabricated by powder injection moulding process. Ceram Int 2019;45(9):11648–53.
[12] Arifin A, Sulong AB, Muhamad N, Syarif J, Ramli MI. Powder injection molding of HA/Ti6Al4V composite using palm stearin as based binder for implant material. Mater Des (1980–2015) 2015;65:1028–34.
[13] Dehghan-Manshadi A, Bermingham Mj, Dargusch MS, StJohn DH, Qian M. Metal injection moulding of titanium and titanium alloys: challenges and recent development. Powder Technol 2017;319:289–301.
[14] Chang I, Zhao Y, editors. Advances in powder metallurgy: properties, processing and applications. Oxford: Woodhead Publishing; 2013.
[15] Yang S, Zhang R, Qu X. Optimization and evaluation of metal injection molding by using X-ray tomography. Mater Char 2015;104:107–15.
[16] Hangai Y, Takahashi K, Yamaguchi R, Utsunomiya T, Kitahara S, Kuwazuru O, et al. Nondestructive observation of pore structure deformation behavior of functionally graded aluminum foam by X-ray computed tomography. Mater Sci Eng 2012;556:678–84.
[17] Selcuk C. Non-Destructive evaluation of powder metallurgy parts. Adv Powder Metallurgy 2013:437–54. Elsevier.
[18] James, W. B., "Powder metallurgy methods and applications," p. 11.
[19] De Chiffre L, Carmignato S, Kruth J-P, Schmitt R, Weckenmann A. Industrial applications of computed tomography. CIRP Annals 2014;63(2):655–77.
[20] Huang B, Liang S, Qu X. The rheology of metal injection molding. J Mater Process Technol 2003;137(1):132–7.
[21] Landis EN, Keane DT. X-ray microtomography. Mater Char 2010;61(12):1305–16.
[22] Tsarouchas D, Markaki AE. Extraction of fibre network architecture by X-ray tomography and prediction of elastic properties using an affine analytical model. Acta Mater 2011;59(18):6989–7002.
[23] Isaac A, Sket F, Reimers W, Camin B, Sauthoff G, Pyzalla AR. In situ 3D quantification of the evolution of creep cavity size, shape, and spatial orientation using synchrotron X-ray tomography. Mater Sci Eng 2008;478(1–2):108–18.
[24] Kastner J, Harrer B, Degischer HP. High resolution cone beam X-ray computed tomography of 3D-microstructures of cast Al-alloys. Mater Char 2011;62(1):99–107.
[25] Olmos L, Bouvard D, Salvo L, Bellet D, Di Michiel M. Characterization of the swelling during sintering of uniaxially pressed copper powders by in situ X-ray microtomography. J Mater Sci 2014;49(12):4225–35.
[26] Weber O, Rack A, Redenbach C, Schulz M, Wirjadi O. Micropowder injection molding: investigation of powder-binder separation using synchrotron-based microtomography and 3D image analysis. J Mater Sci 2011;46(10):3568–73.
[27] Heldele R, Rath S, Merz L, Butzbach R, Hagelstein M, Haußelt J. X-ray tomography of powder injection moulded micro parts using synchrotron radiation. Nucl Instrum Methods Phys Res Sect B Beam Interact Mater Atoms 2006;246(1):211–6.
[28] Fang W, He X, Zhang R, Yang S, Qu X. "The effects of filling patterns on the powder–binder separation in powder injection molding. Powder Technol 2014;256:367–76.
[29] Zoya ZA, Krishnamurthy R. The performance of CBN tools in the machining of titanium alloys. J Mater Process Technol 2000;100(1–3):80–6.
[30] Rahman M, Wang Z-G, Wong Y-S. A review on high-speed machining of titanium alloys. JSME Int J, Ser C 2006;49(1):11–20.
[31] Hsu RW-W, Yang C-C, Huang C-A, Chen Y-S. "Electrochemical corrosion properties of Ti–6Al–4V implant alloy in the biological environment. Mater Sci Eng 2004;380(1–2):100–9.
[32] Reclaru L. Corrosion behavior of a welded stainless-steel orthopedic implant. Biomaterials 2001;22(3):269–79.
[33] Case Study - DIRA-GREEN. The importance of an IP management structure in a research project. https://www.iprhelpdesk.eu/sites/default/files/newsdocuments/CS-Importance-of-IP-management-structure-for-research-projects.pdf".

[34] Baruchel J, Buffiere JY, Maire E. X-ray tomography in material science. France: Hermes science publications; 2000.
[35] Buffiere JY, Maire E, Adrien J, Masse JP, Boller E. In situ experiments with X ray tomography: an attractive tool for experimental mechanics. Exp Mech 2010;50(3):289–305.
[36] Maire E, Withers PJ. Quantitative X-ray tomography. Int Mater Rev 2014;59(1):1–43.
[37] Du Plessis A, Yadroitsava I, Yadroitsev I. Effects of defects on mechanical properties in metal additive manufacturing: a review focusing on X-ray tomography insights. Mater Des 2020;187:108385.
[38] Arifvianto B, Leeflang MA, Zhou J. Characterization of the porous structures of the green body and sintered biomedical titanium scaffolds with micro-computed tomography. Mater Char 2016;121:48–60.
[39] Urtekin L, Usta Y. The importance of dıgıtal radiography in metal injection molding method. Bilecik Seyh Edebali Univ J Sci 2018:82–8.
[40] Urtekin L, Taşkın A. Ti–6Al–4V alloy cortical bone screw production by powder injection molding method. MEX 2017;7(4):245–52.
[41] Muchavi NS. X-ray computed microtomography studies of MIM and DPR parts. J South Afr Inst Min Metall 2016;116(10):973–80.
[42] Urtekin L. Investigation of the effect of molding and sintering parameters on properties of powder injection molded steatite ceramics. Ph. D. Thesis. Gazi University; 2008.
[43] Urtekin L, Uslan İ, Tuç B. Investigation of effect of feedstock rheologies for injection molding of steatite. J Faculty Eng Arch Gazi University 2012;27(2):333–41.